THE JOURNAL OF PHYSICAL CHEMISTRY A

Article

pubs.acs.org/JPCA

Trends in Bond Dissociation Energies of Alcohols and Aldehydes Computed with Multireference Averaged Coupled-Pair Functional Theory

Victor B. Oyeyemi,[†] John A. Keith,[‡,⊥] and Emily A. Carter*[,‡,§,∥]

[†]Department of Chemical and Biological Engineering, [‡]Department of Mechanical and Aerospace Engineering, [§]Program in Applied and Computational Mathematics, and [∥]Andlinger Center for Energy and the Environment, Princeton University, Princeton, New Jersey 08544, United States

Supporting Information

ABSTRACT: As part of our ongoing investigation of the combustion chemistry of oxygenated molecules using multireference correlated wave function methods, we report bond dissociation energies (BDEs) in C1−C4 alcohols (from methanol to the four isomers of butanol) and C1−C4 aldehydes (from methanal to butanal). The BDEs are calculated with a multireference averaged coupled-pair functional-based scheme. We compare these multireference BDEs with those derived from experiment and single-reference methods. Trends in BDEs for the alcohols and aldehydes are rationalized by considering geometry relaxations of dissociated radical fragments, resonance stabilization, and hyperconjugation. Lastly, we discuss the conjectured association between bond strengths and rates of hydrogen abstraction by hydroxyl radicals. In general, abstraction reaction rates are higher at sites where the C−H bond energies are lower (and vice versa). However, comparison with available rate data shows this inverse relationship between bond strengths and abstraction rates does not hold at all temperatures.

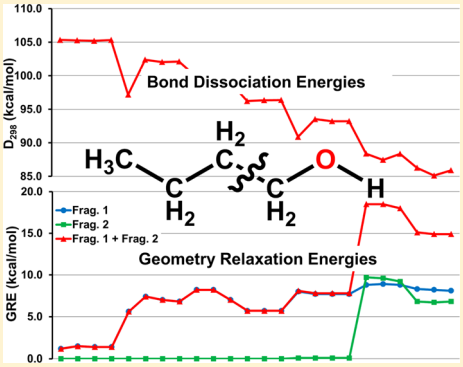

1. INTRODUCTION

Alcohols and aldehydes play important roles in many areas of chemistry, including combustion. Relatively short-chain alcohols (e.g., those ranging from methanol to butanol) can be used as liquid transportation fuels for internal combustion engines[1] and in fuel cells (as in the case of methanol).[2,3] Alcohols are attractive biorenewable fuels because they can be produced from plant sources such as simple and complex sugars, biomass, and biological waste products.[1,4] Their combustion is theoretically CO_2-neutral because their biological synthesis consumes atmospheric CO_2. As with other oxygenated fuels, alcohols release less soot and other pollutants than crude-oil-derived fuels. Aldehydes, on the other hand, are not used as fuels in combustion but rather as additives and promoters,[5] and they are sometimes toxic air pollutants.[6] Because alcohol combustion generates aldehydes,[7−10] understanding how to limit their generation from otherwise clean-burning alcohols is a matter of concern.

Chemical kinetics models used to provide insight into fuel combustion typically require bond dissociation energies (BDEs) as inputs (e.g., for calculating enthalpies of formation). Here, we directly compute and analyze alcohol and aldehyde BDEs using ab initio quantum chemistry, complementing our other recent efforts to determine the BDEs of other oxygenated molecules such as acids and esters.[11,12] We analyze BDE trends in a series of alcohols (from methanol through butanols) and aldehydes (from formaldehyde through butanal). We show that the trends can be well rationalized by considering the extent of structural relaxation in the dissociated radicals, along with electronic effects such as resonance stabilization and hyperconjugation.

Multiple reports of theoretically predicted alcohol and aldehyde BDEs exist in the literature. For example, O−C BDEs in alcohols have been derived from density functional theory (DFT) and semiempirical G*n* methods,[13,14] BDEs in vinyl alcohols from CBS-*n* and G*n* methods,[15,16] BDEs for C1−C4 alcohols from semiempirical CBS-QB3 theory within isodesmic schemes,[17] BDEs in isobutanol using DFT and CBS-QB3,[18] and BDEs of normal C1−C5 aldehydes from semiempirical CBS-APNO[19] theory.[20] BDEs are normally computed using single reference ab initio methods, because these methods are often accurate and straightforward to carry out. The approach utilized here is different in that we use a multireference method, specifically the multireference averaged coupled-pair functional (MRACPF2).[21,22] As we discuss at length elsewhere,[11,12] accurate BDEs computed from single-reference methods and from our multireference procedure generally agree, but there are significant differences for a few specific bonds in oxygenated molecules that warrant special attention (vide infra). As done previously, we compare MRACPF2 BDEs to accurate single-reference BDEs for benchmarking purposes. Our motivation for using multireference rather than single reference methods for computing BDEs is to use an accurate method that can be used

Received: February 14, 2014
Revised: April 6, 2014
Published: April 7, 2014

 © 2014 American Chemical Society dx.doi.org/10.1021/jp501636r | *J. Phys. Chem. A* 2014, 118, 3039−3050

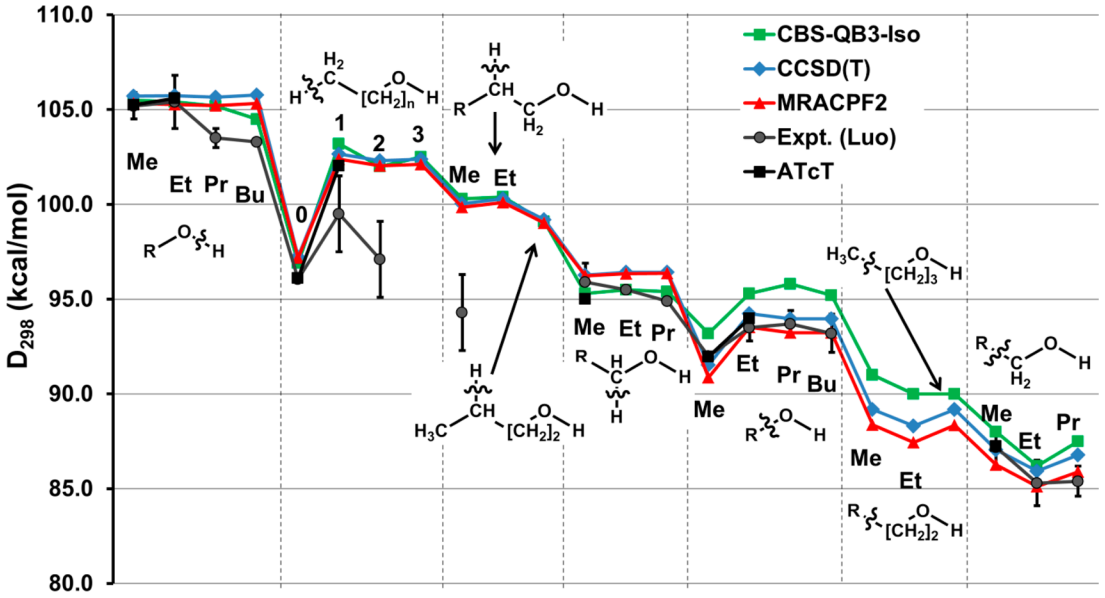

Figure 1. BDEs (D_{298}s) of C1−C4 normal alcohols (methanol, ethanol, *n*-propanol, and *n*-butanol) from MRACPF2, CCSD(T), CBS-QB3-Iso, and reference energies from experiment (Luo[49]) and ATcT. All MRACPF2 BDEs were from CAS(2e,2o)-based calculations. The inset figures denote different breaking bonds where R groups (Me, Et, Pr, Bu) denote the different substituted alcohols and numbers (n = 0−3) denote different alkyl chain lengths.

consistently across an entire potential energy surface; only multireference methods can be used for such a purpose. Benchmarking multireference methods for BDEs, among the few directly measurable quantities available, is therefore critical to future modeling of entire combustion reaction potential energy surfaces.

Besides their use in reaction kinetics models, many researchers use BDEs as thermodynamic descriptors to rationalize dissociation and hydrogen abstraction reaction rates (see, e.g., analyses in ref 17). Below, we test this practice by systematically comparing bond strengths and rates of hydrogen abstraction in butanol isomers, as well as describing the temperature dependence of BDEs.

2. COMPUTATIONAL DETAILS

Our computational approach is described at length elsewhere,[11,12] but we repeat the important elements here. We define D_e (electronic energy change upon dissociation), D_0 (enthalpy of dissociation at 0 K), and D_{298} (enthalpy of dissociation at 298 K) for a generic bond A−B as

$$D_e = \Delta E_{MRACPF2} \quad (1)$$

$$D_0 = D_e + \Delta ZPE \quad (2)$$

$$D_{298} = D_0 + \Delta H_{0\rightarrow 298} \quad (3)$$

where ΔZPE is the zero point energy difference and $\Delta H_{0\rightarrow 298}$ is the thermal correction difference between the dissociated fragments ($A^\bullet$ + $B^\bullet$) and the undissociated molecule (AB), all computed at their optimized equilibrium geometries. Geometries, vibrational frequencies, and ΔZPE and $\Delta H_{0\rightarrow 298}$ energy terms are computed with DFT-B3LYP[23] and a triple-ζ basis set (either 6-311G(2d,p)[24,25] or cc-pVTZ).[26] To account for anharmonicity, frequencies are scaled by the recommended values of 0.99 or 0.985[27] for the respective basis sets. Both basis sets give essentially the same BDEs (Supporting Information, Table S1). We have previously[11] compared D_es calculated from multireference singles and doubles configuration interaction (MRSDCI),[28,29] multireference averaged coupled-pair functional (MRACPF and MRACPF2) methods,[21,22] as well as MRSDCI with the a posteriori size-extensive Davidson−Silver correction (MRSDCI-DS).[30−33] That work showed that our scheme functions most accurately and reliably with MRACPF2 electronic energies. Therefore, only MRACPF2 are results reported here.

The complete active space self-consistent field (CASSCF)[34] method is used as the reference multiconfigurational wave function for the MRACPF2 calculations. Note that CASSCF active space sizes depend on the bond being broken.[11] The CAS(2e,2o) active space consisting of two electrons in two orbitals (σ and σ^*) of the dissociating bond is appropriate for most bonds in alcohols and aldehydes. Important π-electron resonance effects arise in bonds beta (β) to the carbonyl group of aldehydes, and so a CAS(4e,4o) active space, consisting of the π and π^* orbitals of the C═O bond and the σ and σ^* orbitals of the dissociating bond, is needed for quantitatively accurate predictions. CASSCF and MRACPF2 calculations at the dissociated limit are computed with the fragments separated by 10 Å and their energies computed together as a *supermolecule* to retain size consistency. We use a superset of reference configurations consisting of the dominant CASSCF configurations in the equilibrium geometries and supermolecules for the MRACPF2 calculations. The dominant configurations are defined as those with CASSCF wave function coefficients greater than 0.05. Superset CAS(2e,2o) reference configurations used are $\sigma\sigma^*$ = 20 and 02 from the equilibrium geometry and XY=11 from the supermolecule, where X and Y represent the orbitals at respective radical centers. Superset CAS(4e,4o) reference configurations used are $\sigma\sigma^*\pi\pi^*$ = 2020, 2002, and 0220 from the equilibrium geometry and (2p)(X)$\pi\pi^*$ = 1120, 1111, 1102, and 2101 from the supermolecule, where 2p is the singly occupied π−radical orbital on the C═O-containing allyl-like radical and X stands for either the hydrogen 1s or the 2p-like orbital of an alkyl radical. The use of superset references provides consistency to the calculations by preserving the number of

dx.doi.org/10.1021/jp501636r | J. Phys. Chem. A 2014, 118, 3039−3050

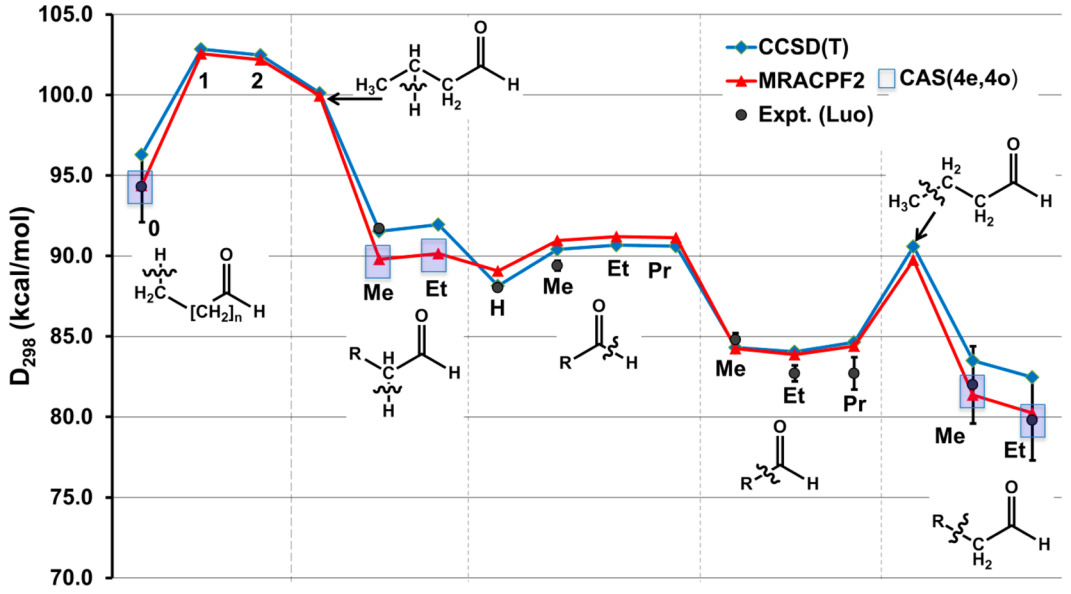

Figure 2. BDEs (D_{298}s) of C1−C4 normal aldehydes (formaldehyde, acetaldehyde, propanal, *n*-butanal) from MRACPF2, CCSD(T), and experimental energies from Luo.[49] MRACPF2 energies from CAS(4e,4o) references are designated with shaded boxes. All others were obtained with CAS(2e,2o) reference spaces. Inset figures denote different breaking bonds where R groups (Me, Et, Pr) denote the different substituted aldehydes and numbers (n = 0−3) denote different alkyl chain lengths.

excitations for the undissociated and supermolecule geometries. We choose the more stringent CASSCF configuration selection threshold of 0.05 because a looser one of 0.1 will leave out important configurations and lead to erroneous BDEs.

The dynamic correlation energy is the difference between the MRACPF2 energy and the reference energy ($E^{corr} = E^{MRACPF2} - E^{ref}$). E^{ref} is used in the MRACPF2 equations and there are two choices to define the reference energy. The first defines it as the CASSCF energy and the second as the energy of a small CI computed within the space of reference configurations used in the CI. This *reference CI energy* is exactly the CASSCF energy when all CASSCF configurations are used as references (e.g., for calculations using CAS(2e,2o) active spaces). The CASSCF and reference CI energies are different when a subset of the CASSCF configurations is used as references in the MRACPF2 calculation. For example, in the CAS(4e,4o) calculations reported here, we use 7 reference configuration state functions (CSFs) out of a possible 20 CSFs; the reference CI energy difference in each case is only ∼1.5 mHartrees. For consistency, we used the subset reference CI energies in the MRACPF2 equations. We extrapolated the reference energies (E^{ref}) and the correlation (E^{corr}) energies to the complete basis set limit using cc-pVDZ (X = 2) and cc-pVTZ (X = 3) basis sets with the scheme:[35−37]

$$E_X^{ref} = E_X^{ref} + A^{ref} X^{-3.4} \quad (1a)$$

$$E_X^{corr} = E_X^{corr} + A^{corr} X^{-2.4} \quad (2a)$$

Note that we find that the two choices of reference energies (subset of or all CSFs) give identical BDEs (within 0.1 kcal/mol) after basis set extrapolation, provided the coefficient threshold used to select references from CASSCF configurations is sufficiently large (e.g., 0.05) such that we do not leave out important configurations.

CASSCF computations were performed within MOLCAS[38] while TigerCI[39−43] was used for MRACPF2 calculations. We compare MRACPF2 BDEs with BDEs from single-reference coupled cluster singles and doubles with perturbative triples (CCSD(T))[44] theory for benchmarking purposes. The CCSD(T) calculations were done with the same cc-pVDZ/cc-pVTZ basis set extrapolation used for MRACPF2 and were performed within MOLPRO.[45]

3. COMPARISON OF MRACPF2 NORMAL ALCOHOL AND ALDEHYDE BDES WITH THOSE FROM SINGLE REFERENCE METHODS, ACTIVE THERMOCHEMICAL TABLES, AND EXPERIMENTS

We begin by comparing D_{298}s from MRACPF2 theory to those from experiments and single reference CCSD(T) and "CBS-QB3-Iso" theories (Figures 1 and 2). We aim for chemical accuracy in our calculations, where chemical accuracy is defined as accuracy of 1 kcal/mol or better in comparison with a reliable reference. Figure 1 displays BDEs of the four normal C1−C4 alcohols (methanol, ethanol, *n*-propanol, and *n*-butanol) grouped according to bond type. MRACPF2, CCSD(T), and reference BDEs are shown along with CBS-QB3-Iso data,[17] which uses CBS-QB3[46] reaction energies obtained from isodesmic schemes to maximize error cancellation.[47,48] The experimental reference D_{298}s ("Expt. (Luo)") come from the extensive compilation of Luo.[49] This data set lists each BDE with as many as five different values from multiple experimental sources. The resulting imprecision necessitates some caution regarding the reliability of the recommended values plotted in the figures. The second set of reference BDEs ("ATcT") are derived from enthalpies of formation of molecules and radicals from the Active Thermochemical Tables (ATcT):[50−52] $D_0 = \Delta H_f^0(A) + \Delta H_f^0(B) - \Delta H_f^0(AB)$. From the ATcT data, we derived D_0s and added DFT-B3LYP $\Delta H_{0\rightarrow 298}$ values to obtain what we treat as benchmark D_{298}'s. ATcT enthalpies are presumed to be very accurate with uncertainties less than 0.2 kcal/mol; therefore, derived D_{298}s values should also be quite accurate. However, not enough ATcT data exist to make as comprehensive a reference set as the Luo compilation.

Experimental and ATcT BDEs differ for some bonds, particularly those in the H−$CH_2[CH_2]_n$OH (n = 0−3) bond

dx.doi.org/10.1021/jp501636r | J. Phys. Chem. A 2014, 118, 3039−3050

group. In the instances where ATcT data are available, computed D_{298}'s tend to agree better with ATcT D_{298}s.

For BDEs involving HOCH(R)−H, R−OH, and R−CH_2OH bonds, reference, CCSD(T), and MRACPF2 BDEs have an average deviation relative to MRACPF2 within 1 kcal/mol. On the other hand, for RO−H and H−$CH_2[CH_2]_n$OH bonds, ATcT and the computed values disagree more substantially with Luo's experimental compilation. Based on the general agreement between different calculations and ATcT data, we conclude that the experimental data are suspect in these cases, especially the anomalously low experimental BDE values for the β and terminal C−H bonds in *n*-propanol.

As stated earlier, multiple experimental data are available for some bonds, making it challenging to determine which of the data are best for benchmarking. Computed BDEs in turn can be used as validators when multiple experiments show disparity. For example, the D_{298}s and report years (in parentheses) for experimental BDEs of *n*-C_3H_7O−H are 105.9 ± 2 kcal/mol (1973), 103.4 ± 1 kcal/mol (1974), ≤103.5 ± 0.5 kcal/mol (2003), and 103.2 kcal/mol (2005). Computed BDEs (MRACPF2, 105.2 kcal/mol; CCSD(T), 105.6 kcal/mol; CBS-QB3-Iso, 105.2 kcal/mol) seem to agree best with the oldest BDE, while agreeing less well with the three newer BDEs, which are all quite similar. Given that the calculated D_{298}s of two homologous bonds CH_3O−H and CH_3CH_2O−H agree with the experimental and ATcT references (∼105.5 kcal/mol), we conclude that the somewhat lower experimental D_{298}s for $CH_3CH_2CH_2O$−H (and $CH_3CH_2CH_2CH_2O$−H) are less accurate.

A more detailed comparison of computed energies shows that C−H and O−H BDEs predicted by MRACPF2 are in very good agreement with those from CCSD(T). MRACPF2 D_{298}s are generally lower than CCSD(T) D_{298} by 0.4 kcal/mol for O−H bonds, by 0.3 kcal/mol for terminal C−H bonds (0.1 for methanol), by 0.1 kcal/mol for C−H bonds α to O, and by 0.2 kcal/mol for secondary C−H bonds beyond the α position to O. BDEs of C−C and O−C bonds predicted by CCSD(T) and MRACPF2 show somewhat larger differences. MRACPF2 energies are lower than CCSD(T) energies by 0.6−0.7 kcal/mol for O−C bonds and by 0.8−0.9 kcal/mol for C−C bonds. Recall that in our scheme, MRACPF2 and CCSD(T) calculations use the same geometries and vibrational frequencies, so the differences between these two methods here are attributable solely to differences in the CCSD(T) and CAS(2e,2o)-MRACPF2 electronic energies. Overall, CCSD(T) and MRACPF2 predict very similar BDEs for bonds in alcohols.

CBS-QB3 is a composite model chemistry scheme based on Møller−Plesset perturbation theory (MP2 and MP4) and CCSD(T) energies. Its energies are designed to approach the complete basis set and all-electron limits, while utilizing empirically derived parameters for two-electron and spin correction terms. CBS-QB3 uses DFT-B3LYP/6-311G(2d,p) geometries and vibrational frequencies, as we have done here for our CCSD(T) and MRACPF2-based calculations. However, the CBS-QB3-Iso data presented for comparison in Figure 1 were obtained with isodesmic error cancellation schemes, which are not necessarily unique and may produce different energies, depending on the choice of reaction selected for the reference enthalpies in the isodesmic scheme. We observe (Figure 1) that CCSD(T) BDEs agree better with MRACPF2 BDEs than with CBS-QB3-Iso BDEs. Disagreements between CBS-QB3-Iso and MRACPF2 D_{298}s are less than 0.3 kcal/mol for most O−H bonds, except for $CH_3CH_2CH_2CH_2O$−H where the disagreement is 0.8 kcal/mol. We conclude that the CBS-QB3-Iso D_{298} for $CH_3CH_2CH_2CH_2O$−H is probably too low. Similarly, disagreements between CBS-QB3-Iso and MRACPF2 D_{298}s are less than 0.4 kcal/mol for most non-α C−H bonds, with the exception of H−CH_2CH_2OH where there is a difference of 0.8 kcal/mol. On the other hand, CBS-QB3-Iso D_{298}'s are lower than MRACPF2 D_{298}s by 0.8−1.0 kcal/mol for all α C−H bonds.

Differences in BDEs between CBS-QB3-Iso and MRACPF2 or CCSD(T) are most pronounced for C−C and O−C BDEs, where CBS-QB3-Iso D_{298}'s are higher than MRACPF2 D_{298}s by 1.1−2.6 kcal/mol. The isodesmic schemes seem to reduce errors compared to reference BDEs for C−H and O−H bond energies for all but two cases: $CH_3CH_2CH_2CH_2O$−H and H−CH_2CH_2OH. However, the isodesmic schemes used in the current CBS-QB3-Iso data set appear to be less reliable when applied to C−C and O−C bond breaking.

Figure 2 shows D_{298}s of four aldehydes (formaldehyde, acetaldehyde, propanal, and *n*-butanal) from MRACPF2, CCSD(T), and experiment ("Expt. (Luo)") grouped according to bond type. Note that when bonds β to the carbonyl group dissociate, the resulting radical can experience an allylic-like π-electron resonance stabilization. Thus, BDEs for these β bonds require calculations at the CAS(4e,4o) level to allow such resonance to be described properly, in which C═O π and π^* orbitals are added to the active space in addition to the σ and σ^* orbitals of the dissociating bond.[11] BDEs for the other bonds in these molecules were computed at the CAS(2e,2o) level. As was found for the alcohols reported above, MRACPF2 BDEs computed at the CAS(2e,2o) level (labeled "MRACPF2") and CCSD(T) show very good agreement with each other, with a maximum BDE difference of 1 kcal/mol. Also, as was found for all the alcohol bonds, MRACPF2 D_{298}s for aldehydes are mostly lower than corresponding CCSD(T) D_{298}'s. The only exceptions are the RC(═O)—H bonds, which are the cases where CCSD(T) and CAS(2e,2o)-MRACPF2 energies show the largest differences (0.5−0.9 kcal/mol). For calculations requiring CAS(4e,4o), MRACPF2 energies are substantially lower than CCSD(T) energies, by 2 kcal/mol. The decrease makes sense physically, because the CAS(4e,4o)-MRACPF2 can properly describe the π-resonance stabilization of the radical mentioned above; this final state stabilization lowers the BDE relative to a single-reference method that accounts less well for this stabilization. Overall, there is good agreement between CAS(2e,2o)-MRACPF2, CCSD(T), and experiment for cases where CAS(2e,2o) is sufficient. For cases involving multiconfigurational wave functions requiring at least a CAS(4e,4o), MRACPF2 agrees with nominal experimental BDEs better than nonmulticonfigurational CCSD(T) for three out of four BDEs. However, CCSD(T) BDEs do fall within experimental error bounds.

4. BDE TRENDS AND GEOMETRY RELAXATIONS IN NORMAL ALCOHOLS AND ALDEHYDES

As we shall show, BDE trends shown in Figures 1 and 2 can largely be understood by evaluating the energy changes due to structural relaxation in the dissociated radicals, which we denote as geometry relaxation energies (GREs). The GRE is the energy decrease in the radical fragment(s) after the bond in the parent molecule is broken, due to the change in equilibrium geometry from that of the parent molecule to that of the dissociated radical fragments.[53] Figure 3 depicts the relaxation of the methyl radical as an illustration of the energy change upon C−H bond breaking in methane (CH_4), which undergoes relaxation from a pyramidal

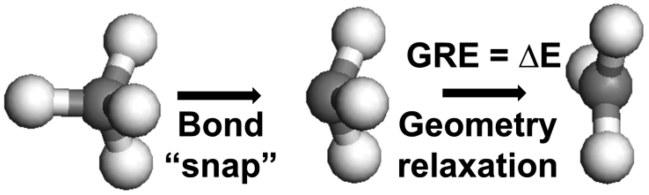

Figure 3. Geometric relaxation energies (GREs) of radicals (methyl radical shown here) following bond snap from parent molecules (methane shown here). See text for further explanation.

to a planar structure. We denote a bond "snap" to mean the thought experiment in which the bond is first broken without any change in geometry other than cleaving the one bond to form the radicals. The radicals are thus momentarily in the geometry they adopted as moieties in the parent molecule. These radicals are then allowed to undergo geometry relaxation and it is the energy difference between the radical in the bond snap geometry and the radical in its equilibrium geometry that is the GRE.

GREs for radicals from different parent molecules (Table 1) relevant to this work were obtained by relaxing, at the unrestricted (U) DFT-B3LYP/6-311G(2d,p) level, the radical structures starting from the geometries they assume within UDFT-B3LYP/6-311G(2d,p)-optimized equilibrium geometries of the parent molecules. One might wonder about possible effects of dispersion interactions not captured by DFT-B3LYP that might affect the GREs. To assess this possibility, we also computed GREs with UCCSD(T)/cc-pVTZ using single point energies at UDFT-B3LYP geometries (because CCSD(T) geometry optimization on larger molecules is prohibitively expensive). GREs from UDFT-B3LYP and UCCSD(T) show similar trends. UDFT-B3LYP GREs are larger than UCCSD(T) GREs by an average of 0.2 and 0.5 kcal/mol for alcohol and aldehyde radicals, respectively (Supporting Information Figures S1 and S2). Thus, as expected, dispersion interactions in these small molecules are fairly small, and the UDFT-B3LYP GREs appear sufficient for the qualitative analyses that follow.

Table 1 shows that there is only a slight size dependence of GREs for homologous fragments (see alkyl radicals, left columns). For example, GREs for alkyl radicals in **R**CH_2−H (where **R** = methyl, ethyl, or propyl) are quite consistently between 6.8 and 6.9 kcal/mol. A similar trend holds for alkyl radicals from other parent molecules, with the range in GREs being at most 0.3 kcal/mol (for R−OH). The GRE of any radical depends on the degree of steric interactions that the radical atoms experienced while embedded within the parent molecule. Alkyl radicals, for instance, have GREs of ∼6.9 kcal/mol when they come from C−H bond breaking in **R**CH_2−H, but they have GREs of ∼9.0 kcal/mol when they originate from C−C bond breaking in R−CH_3. Also, a particular radical may have different relaxation energies depending on the molecule type: alkyl radicals in R−CH_3 and **R**−CH_2OH have slightly different values of ∼9.0 and ∼8.2 kcal/mol, respectively, whereas alkyl radicals in **R**−C(═O)H have GREs of ∼7.6 kcal/mol. Furthermore, even for the same molecule and bond type, GREs may differ depending on the location of the bond relative to a functional group: **R** in **R**−CH_2OH and **R**−$CH_2[CH_2]_n$OH have values of ∼8.2 and ∼8.9 kcal/mol, respectively.

GREs of oxygenated radicals (oxy radicals) are close to those of alkyl radicals if the radical site is a carbon atom and the radical site is at least two atoms away from the oxygenated functional group (Table 1; see oxy radicals, middle columns). For example, the oxy radical formed from primary C−H bond scission in butanol (**HOCH$_2$CH$_2$CH$_2$CH$_2$**−H) has the same GRE as alkyl radicals formed from alkanes (6.8 kcal/mol). GREs increase slightly as the alcohol length shortens in propanol and ethanol (GRE(**HOCH$_2$CH$_2$CH$_2$**−H) = 7.0 kcal/mol and GRE-(**HOCH$_2$CH$_2$**−H) = 7.4 kcal/mol). However, the GRE drops to 5.6 kcal/mol for **HOCH$_2$**−H. **HOC$\underline{H_2}$R** (R = Me−Pr) radicals have similar GREs (5.7 kcal/mol) to **HOCH$_2$**−H, due perhaps to a common hyperconjugation effect (vide infra). Nonprimary radicals **HOCH$_2$C$\underline{H_2}$R** (R = Me, Et) have GREs of 8.2 kcal/mol whereas **HOCH$_2$CH$_2$C$\underline{H_2}$CH$_3$** has a GRE of 7.0 kcal/mol. Similar trends are seen for the aldehyde radicals except that radicals formed from beta H atom scissions have high GREs between 12.7 and 14.6 kcal/mol, presumably due to the changes in bond lengths that occur due to π-resonance in the resulting radicals.

Lastly, the GREs of oxygenated radicals directly involving scissions of oxygen atoms or of aldehydic moieties tend to be much lower than those from carbon atoms (Table 1; see oxy radicals, right column). For example, GREs for **HO**—R, **RO**—

Table 1. Geometric Relaxation Energies of Radicals (in Bold) Following a Bond "Snap" from Their Parent Molecules, Computed at the UDFT-B3LYP/6-311G(2d,p) Level[a]

alkyl radicals		oxy radicals		oxy radicals	
radical and parent molecule	GRE (kcal/mol)	radical and parent molecule	GRE (kcal/mol)	radical and parent molecule	GRE (kcal/mol)
RCH$_2$—H, R = Me−Pr	6.8−6.9	**HOCH$_2$CH$_2$CH$_2$CH$_2$**—H	6.8	**HO**—R, R = H−Bu	0.1
R—CH_3, R = Me−Pr	8.9−9.0	**HOCH$_2$CH$_2$CH$_2$**—H	7.0	**RO**—H, R = Me, Et−Bu	1.2, 1.4−1.5
R—$CH_2CH_2CH_2OH$, R = Me	8.8	**HOCH$_2$CH$_2$**—H	7.4	**HOCH$_2$**—R, R = Me−Pr	6.7−6.8
R—CH_2CH_2OH, R = Me, Et	8.8−8.9	**HOCH$_2$**—H	5.6	**HOCH$_2$CH$_2$**—R, R = Me, Et	9.6−9.7
R—CH_2OH, R = Me−Pr	8.1−8.3	**HOCH$_2$R**, R = Me−Pr	5.7	**HOCH$_2$CH$_2$CH$_2$**—R, R = Me	9.2
R—OH, R = Me, Et−Bu	7.7, 8.0	**HOCH$_2$CH$_2$R**, R = Me, Et	8.2	**HC(═O)**—R, R = H, Me−Pr	0.4, 1.1
R—$CH_2CH_2C(=O)H$, R = Me	8.9	**HOCH$_2$CH$_2$CH$_2$CH$_3$**	7.0	**RC(═O)**—H, R = Me−Pr	0.8
R—$CH_2C(=O)H$, **R** = Me, Et	8.3, 8.5	**HC(═O)CH$_2$CH$_2$CH$_2$**—H	6.8	**HC(═O)CH$_2$**—R, R = Et	12.6
R—C(═O)H, R = Me−Pr	7.5−7.7	**HC(═O)CH$_2$CH$_2$**—H	7.8	**HC(═O)CH$_2$CH$_2$**—R, R = Me	9.0
		HC(═O)CH$_2$CH$_2$CH$_3$	8.0		
		HC(═O)CH$_2$—H	12.7		
		HC(═O)CH$_2$R, R = Me, Et	14.6, 14.3		

[a]The breaking bonds are denoted with a hyphen or an underline (for nonprimary C—H bonds). For H dissociations from nonprimary sites, the dissociated H (underlined) is shown in the formulas to identify the parent molecules, but the GREs are for the (non-hydrogen) radicals. Me = methyl, Et = ethyl, Pr = propyl, and Bu = butyl.

dx.doi.org/10.1021/jp501636r | J. Phys. Chem. A 2014, 118, 3039−3050

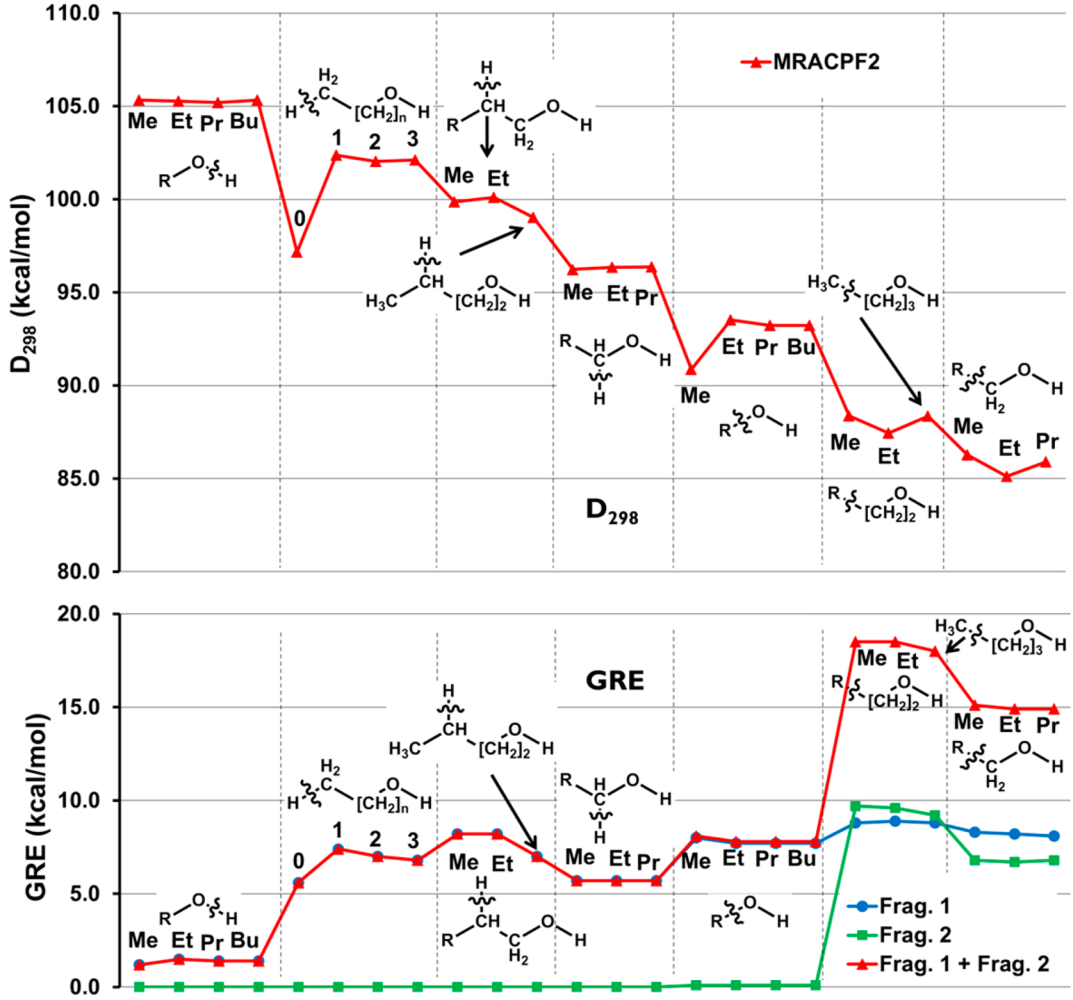

Figure 4. MRACPF2 D_{298}s and UDFT-B3LYP geometry relaxation energies (GREs) of radicals involved in the dissociation of normal alcohol bonds. Radicals on the left-hand side of the breaking bonds (indicated by squiggly lines) are denoted as "Frag 1" and those on the right-hand side as "Frag. 2," but hydrogen atoms are denoted as "Frag. 2" irrespective of their positioning for bond dissociations involving H as a fragment.

H, **HC(=O)**—R, and **RC(=O)**—H are less than or equal to 1.5 kcal/mol, reflecting the fact that these radicals do not relax much upon bond dissociation. By contrast, dissociations resulting in oxygenated alkyl radicals have GREs greater than 6 kcal/mol due to the typical pyramidal to planar relaxation of such radicals. The largest GRE among these oxygenated alkyl radicals is for beta C−C scission that creates an oxyallylic species that has significantly lengthened (shortened) C−O (C−C) bonds due to the π-resonance effect discussed above.

These GREs are reported to help explain trends in BDEs. Figure 4 shows the MRACPF2 D_{298}s (top plot) and UDFT-B3LYP (bottom plot) GREs in a composite plot. The GRE plot displays relaxation energies of the two radical products of bond dissociation, as well as the sum of the two relaxation energies. H and OH do not structurally relax upon dissociation whereas other radicals have GREs of up to 15 kcal/mol. The trend of increasing total GREs mirrors the trend of decreasing BDEs. As expected,[53] the more structural relaxation the radicals undergo after dissociation, the lower the bond energies.

Although GREs explain the primary trend in the BDEs, other factors, particularly hyperconjugation, provide further refinement for understanding BDE trends. For example, within the H−$CH_2[CH_2]_nOH$ group, dissociation in methanol (H−CH_2OH) is easier than dissociation in ethanol through *n*-butanol (H−$\underline{C}H_2[CH_2]_nOH$, n = 1−3) because the $\underline{C}H_2OH$ radical ("_" denotes radical site here and below) is hyperconjugated (the O $2p_\pi$ lone pair electrons partially delocalize into the C $2p_\pi$ singly occupied radical orbital), whereas there is no such effect in the larger radicals ($\underline{C}H_2[CH_2]_nOH$, n = 1−3). The $\underline{C}H_2OH$ radical has a lower GRE than the other radicals ($\underline{C}H_2[CH_2]_nOH$, n = 1−3) and this should normally result in a higher BDE for H−CH_2OH. However, hyperconjugation effects counter this geometric relaxation and effectively lower the bond strength. Similarly, R−CH_2OH bonds are weaker than R−$CH_2[CH_2]_nOH$ because of hyperconjugation in $\underline{C}H_2OH$. Likewise, RCH(OH)−H bonds are weaker than other C−H bonds because of hyperconjugation in R$\underline{C}$H(OH), though, as before, the lower degree of geometry relaxation of R$\underline{C}$H(OH) would have produced the opposite trend to the one caused by hyperconjugation.

Other trends are more challenging to explain. In the R−OH bond group, CH_3−OH is weaker than R−OH (for R = ethyl through butyl) by 2.5 kcal/mol, even though GREs are nearly constant for all four bonds and there is no hyperconjugative stabilization of the CH_3−OH radicals. UDFT-B3LYP and UCCSD(T) predict near-constant total GREs of 7.8−8.1 kcal/mol (MeOH 8.1 kcal/mol; EtOH, PrOH, BuOH 7.8 kcal/mol) and 7.3−8.0 kcal/mol (MeOH 8.0 kcal/mol; EtOH, PrOH,

dx.doi.org/10.1021/jp501636r | J. Phys. Chem. A 2014, 118, 3039−3050

Table 2. Mulliken Charges (CASSCF) for HO−R Bond Breaking[a]

breaking bond	Mulliken charges at atom centers														
$HO-CH_3$	H	O	C	H	H	H									
equ	0.22	−0.39	−0.03	0.05	0.05	0.09									
sup	0.26	−0.26	−0.38	0.12	0.12	0.13									
$HO-CH_2CH_3$	H	O	C	H	H	C	H	H	H						
equ	0.22	−0.40	0.06	0.06	0.08	−0.28	0.09	0.10	0.07						
sup	0.26	−0.26	−0.31	0.13	0.13	−0.24	0.09	0.09	0.09						
$HO-CH_2CH_2CH_3$	H	O	C	H	H	C	H	H	C	H	H	H			
equ	0.22	−0.39	0.05	0.09	0.05	−0.17	0.10	0.07	−0.30	0.09	0.10	0.09			
sup	0.26	−0.26	−0.33	0.14	0.13	−0.11	0.09	0.09	−0.28	0.09	0.10	0.09			
$HO-CH_2CH_2CH_2CH_3$	H	O	C	H	H	C	H	H	C	H	H	C	H	H	H
equ	0.22	−0.39	0.05	0.06	0.09	−0.18	0.10	0.07	−0.18	0.09	0.09	−0.29	0.09	0.09	0.10
sup	0.26	−0.26	−0.034	0.13	0.14	−0.12	0.09	0.09	−0.16	0.09	0.09	−0.29	0.09	0.09	0.10

[a]Atoms are written in the order they appear in the chemical formula. "equ" refers to the undissociated equilibrium geometry and "sup" refers to the supermolecule geometry (with radical fragments in their equilibrium structures). The dash denotes the breaking bond.

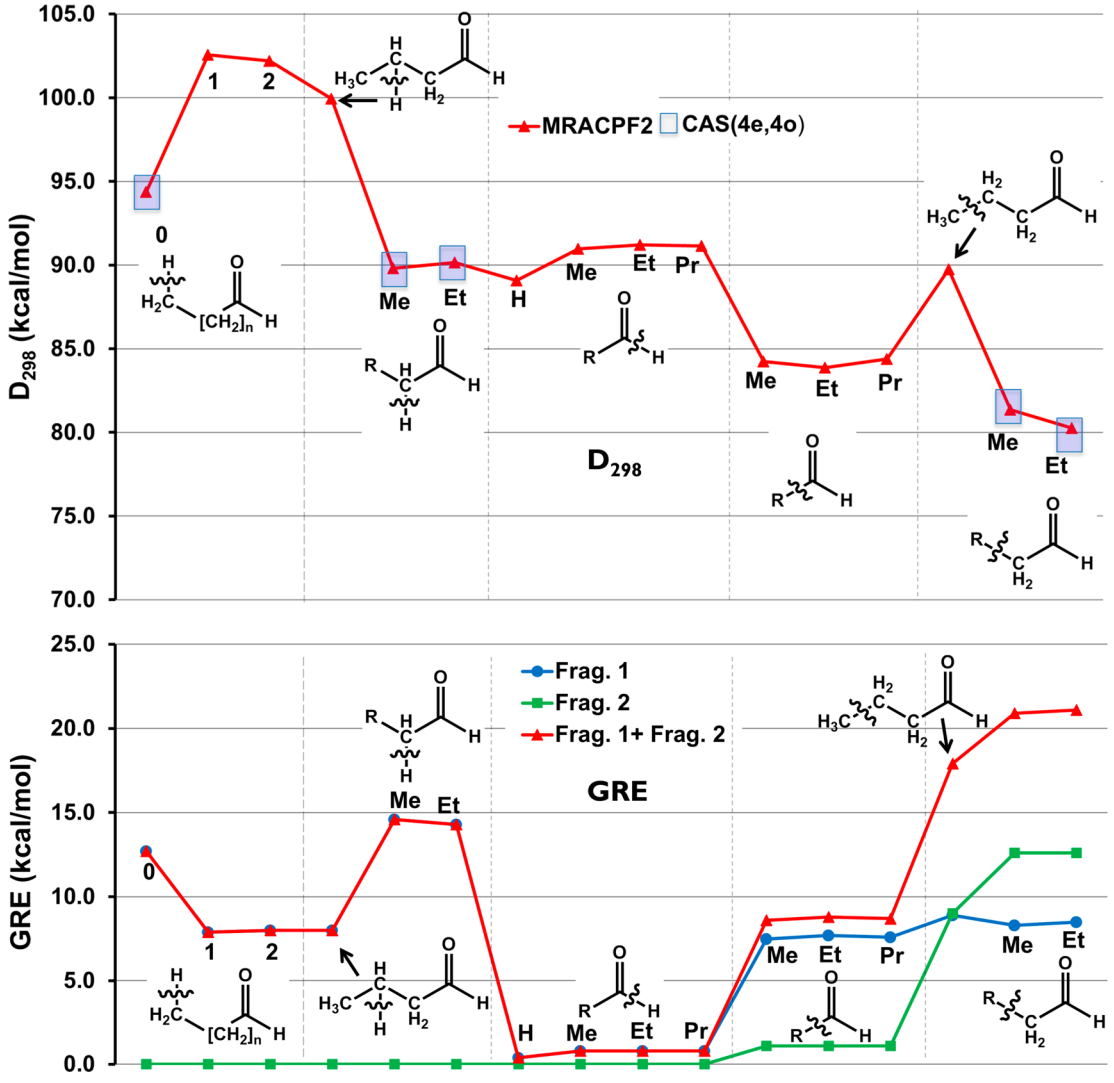

Figure 5. MRACPF2 D_{298}s and UDFT-B3LYP geometry relaxation energies (GREs) of radicals involved in the dissociation of normal aldehyde bonds. Radicals on the left-hand side of the breaking bonds are denoted as "Frag 1" and those on the right-hand side as "Frag 2," but hydrogen atoms are denoted as "Frag 2" irrespective of their positioning for bond dissociations involving H as a fragment.

BuOH 7.3−7.5 kcal/mol), respectively. Although the GRE of MeOH is slightly larger, this does not fully explain the 2.5 kcal/mol BDE difference. Another possible explanation is given by analyzing charges on atoms and considering their relative Pauling electronegativities. Mulliken (CASSCF) charges at atomic positions for both undissociated equilibrium molecules and the supermolecules are shown in Table 2. Focusing on the atoms in the C−O breaking bond, the Mulliken charges show that charge

dx.doi.org/10.1021/jp501636r | J. Phys. Chem. A 2014, 118, 3039−3050

on O accumulates more when bound to C in the undissociated molecule. Likewise, this C atom accumulates more charge when bound to three H atoms (in methanol) rather than two H atoms and an alkyl group (in higher alcohols). The net negative charge on the C atom in methanol may cause some Coulomb repulsion with the net negative charge on the O atom, thereby slightly destabilizing the C−O bond in methanol more than in the higher alcohols. A similar trend and explanation is offered in an earlier publication of Coote et al.[13]

Additional unexplained trends are within the accuracy limit of the calculations. $CH_3CH(CH_2CH_2OH)-H$ is weaker than $CH_3CH(CH_2OH)-H$ and $CH_3CH_2CH(CH_2OH)-H$ by 1 kcal/mol, even though its GRE is lower (Figure 4). Also, $CH_3CH_2-CH_2CH_2OH$ is weaker than $CH_3-CH_2CH_2OH$ and $CH_3-CH_2CH_2CH_2OH$ by 1 kcal/mol despite having very similar GREs. Lastly, $CH_3CH_2-CH_2OH$ is weaker than CH_3-CH_2OH and $CH_3CH_2CH_2-CH_2OH$ by 1 kcal/mol despite having essentially identical GREs. The 1 kcal/mol differences in all of these cases are within the cumulative uncertainties in the calculations.

We next carry out a similar analysis for aldehydes. Figure 5 shows MRACPF2 BDEs and GREs for bond breaking in those molecules. GRE trends largely mirror BDE trends, just as in the case of alcohols. Here resonance stabilization explains trends counter to what would be expected simply from differences in geometry relaxations. Bonds β to the C═O are resonance-stabilized and therefore have significantly lower bond strengths than other bonds in their group: the $H-CH_2C(=O)H$ BDE is lower than $H—CH_2CH_2C(=O)H$ and $H—CH_2CH_2CH_2C(=O)H$ BDEs by ∼8 kcal/mol, $CH_3CH[C(=O)H]—H$ and $CH_3CH_2CH[C(=O)H]—H$ BDEs are lower than the $CH_3CH-[CH_2C(=O)H]—H$ BDE by ∼10 kcal/mol, and $CH_3—CH_2C(=O)H$ and $CH_3CH_2—CH_2C(=O)H$ BDEs are lower than the $CH_3—CH_2CH_2C(=O)H$ BDE by ∼9 kcal/mol. Explanation for other trends are more elusive. Specifically, it is not clear why HC(═O)—H is weaker than RC(═O)—H for R = CH_3, CH_3CH_2, and $CH_3CH_2CH_2$ by ∼2 kcal/mol. An analysis of the Mulliken charges shows that the carbonyl oxygen draws only very slightly more charge from R (∼0.03) than it does from H (Supporting Information Table S2). It is unlikely that this minute difference would explain the stabilization of HC(═O). We also have no evidence of any large structural changes in the resulting formyl/acyl radicals, which might have indicated stabilization stemming from delocalization into the in-plane π-system.

5. BDE VALUES IN ISOPROPANOL AND BUTANOL ISOMERS AND THEIR RELATION TO HYDROGEN ABSTRACTION RATES

We now present and analyze MRACPF2 D_{298}'s (Figure 6) in *iso*-propanol and the four butanol isomers (*n*-butanol, *sec*-butanol, *iso*-butanol, and *tert*-butanol); the normal alcohol D_{298}'s discussed earlier are displayed again for ease of comparison. We make several observations on BDE trends resulting from structural differences. The D_{298} of an O−H bond is 1−2 kcal/mol higher when the oxygen is attached to a secondary or tertiary carbon, as in the cases of *iso*-propanol, *tert*-butanol, and *sec*-butanol (O−H D_{298} ∼ 106.4 kcal/mol), than when it is attached to a primary carbon, as in the cases of methanol, ethanol, *n*-butanol, *iso*-butanol (O−H D_{298} ∼ 105.4 kcal/mol), and *n*-propanol (104.6 kcal/mol). Thus, H abstraction from OH groups bound to primary carbons should be slightly easier. Most terminal methyl C−H bonds of these alcohols have D_{298}s

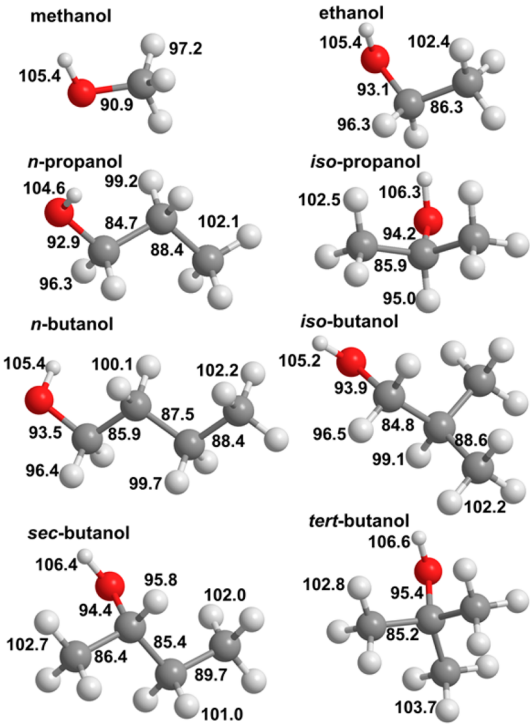

Figure 6. MRACPF2 D_{298}s of C1−C4 alcohol isomers. BDEs for structurally unique bonds are shown for each molecule.

between 102.0 and 102.8 kcal/mol. However, in *tert*-butanol, C−H bonds of the methyl group coplanar with the O−H bond have a higher D_{298} of 103.7 kcal/mol, presumably due to hydrogen bonding to the oxygen lone pair. Some kinetics studies consider all nine C−H bond sites in *tert*-butanol equivalent with regard to hydrogen abstraction.[54] The 1 kcal/mol BDE difference suggests, however, that abstractions from the three C−H sites of methyl within OH plane are equivalent and are different from abstractions from the six equivalent out-of-plane C−H bonds. Yet, the experimentally observed H-abstraction rate will be an average over the nine sites, and thus any of the sites may be indistinguishable from the others. Lastly, we note that C−H bonds α to the OH group in all of these alcohols are uniformly ∼96 kcal/mol due to hyperconjugation; these are the weakest bonds involving hydrogen and are therefore expected to be the most probably sites for initiation of hydrogen abstraction reactions.

Beyond BDEs related to hydrogen abstraction, we consider the C−O and C−C bond strengths for these alcohols as well. The data in Figure 6 suggest that the C−O bond in methanol is weaker than C−O bonds in the larger alcohols by 2−4.5 kcal/mol, despite the GRE for methanol being slightly smaller than for the higher alcohols (vide supra). Variability of C−O D_{298}s in alcohols larger than methanol (92.9−95.4 kcal/mol) follows an easily identifiable pattern, in which C−O bonds involving primary CH_2 groups are slightly weaker (∼93 kcal/mol) than those involving secondary CH(R) groups (∼94 kcal/mol), and with the largest C−O BDE found for *tert*-butanol. The C−C bonds are the weakest of all bonds in the alcohols, ∼85−90 kcal/mol, and those that are α to oxygen are weakest of all: consistently ∼85−86 kcal/mol, again due to hyperconjugative stabilization in the resulting CH_2OH radical. In *sec*-butanol, which contains two unique α C−C bonds, the BDE involving only secondary carbon atoms is weaker by 1 kcal/mol. C−C bonds further away from the OH group are significantly stronger,

dx.doi.org/10.1021/jp501636r | J. Phys. Chem. A 2014, 118, 3039−3050

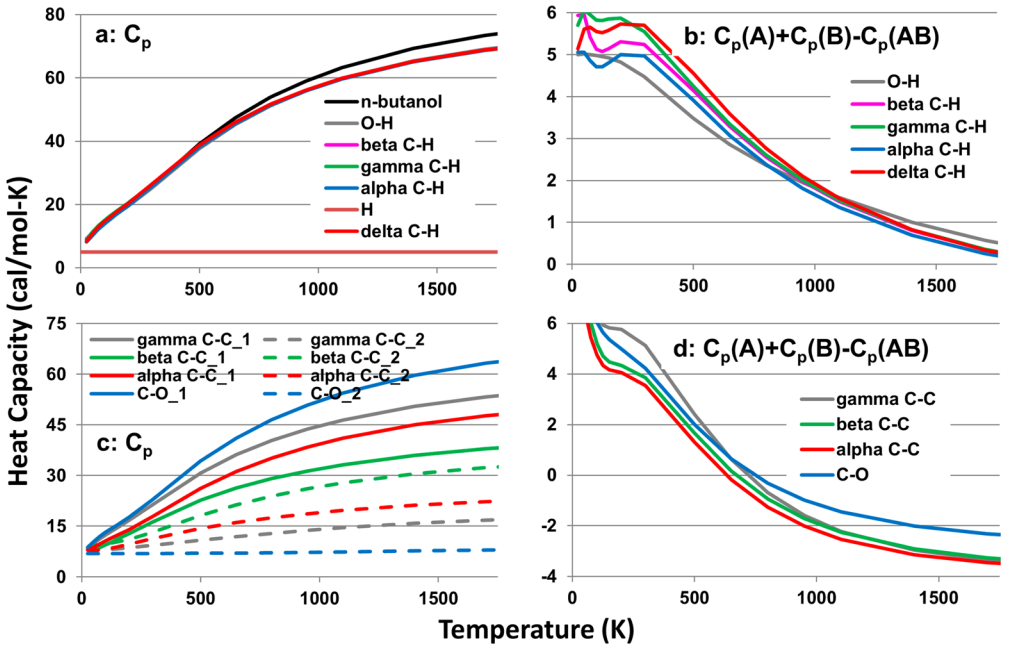

Figure 7. Heat capacities (C_p) of normal butanol and its dissociation products. The left panel shows heat capacities of individual species and the right panel depicts the difference between the sum of heat capacities of the two radical products and *n*-butanol for each bond (A−B → A + B). On the top-left panel, "C−H" denotes alkyl radicals after hydrogen is removed from respective bond sites. The heat capacities of the radicals formed after H-scission are similar and are superimposed in the plot. Lower left panel shows radicals from C−C and C−O bond breaking at sites indicated where "_1" labels alkyl radicals and "_2 " labels oxygen-containing fragments.

consistently ∼89 kcal/mol, because of the lack of electronic stabilization of the resulting radicals. Thus, pyrolytic cleavage is expected to initiate at the C−C bonds α to the OH group.

Thermochemical data used in combustion modeling are needed over a wide temperature range. Temperature dependence of the BDEs is contained within $\Delta H_{0\rightarrow T}$, the thermal correction contribution, and is given for bond AB → A + B as

$$D_T = D_e + \Delta\mathrm{ZPE} + \Delta H_{0\rightarrow T} \tag{3a}$$

$$\Delta H_{0\rightarrow T} = \int_0^T \{C_p(\mathrm{A}) + C_p(\mathrm{B}) - C_p(\mathrm{AB})\}\, dt \tag{4}$$

where C_p(AB) is the heat capacity of molecule AB and C_p(A) and C_p(B) are heat capacities of dissociated radicals A and B. The heat capacities are computed within the ideal gas, rigid rotor, and harmonic oscillator approximations.[55] Figure 7 shows on the left-hand side the predicted heat capacities of *n*-butanol and its corresponding radicals formed upon dissociation of the bonds indicated (Figure 7a, top left panel, C−H and O−H bonds; Figure 7c, bottom left panel, C−C and O−C bonds). The right panels (Figure 7b,d) show differences in heat capacities between the radical fragments and *n*-butanol (i.e., C_p(A) + C_p(B) − C_p(AB)). Heat capacities rise with temperature and plateau at higher temperatures for all species except for the constant value of 5.0 cal/(mol K) of H. Heat capacities of the radicals formed after H-scission are similar at all temperatures, and they differ increasingly from the heat capacity of *n*-butanol only as the temperature rises. Heat capacity differences for all bonds fall steadily and plateau as well for all bonds, with limiting values at 1750 K for C−C and C−O bonds of about −2.5 and −3.5 cal/(mol K), respectively, whereas those for O−H and C−H bonds are negligible (∼0 cal/(mol K)). Integrations under these heat capacity difference profiles determine the thermal contributions to BDEs.

Figure 8 shows our predicted BDEs ($D_T = D_e$ + ΔZPE + $\Delta H_{0\rightarrow T}$) of bonds in *n*-butanol from 0 to 1750 K. BDEs initially

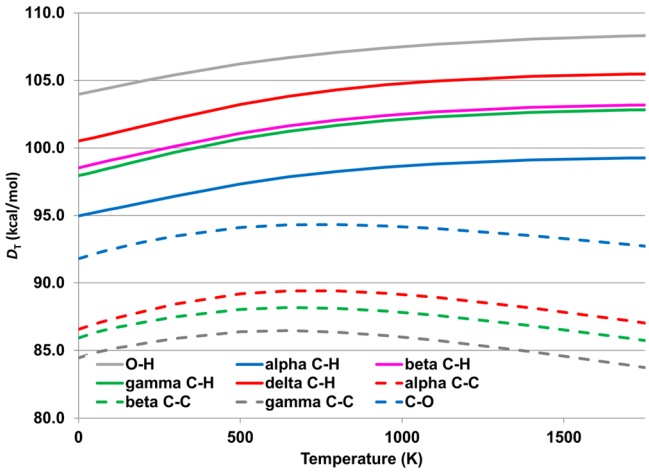

Figure 8. MRACPF2 D_Ts of hydrogen atom dissociations in *n*-butanol isomers for temperatures between 0 and 1750 K.

rise steadily as the temperature increases but eventually decrease at higher temperature for all bonds. The decrease in BDE with temperature for C−H and O−H bonds is subtle and the profiles appear to have plateaued after 700 K. C−C and C−O bonds on the other hand have distinct maximum BDEs at around 700 K. Again, these behaviors are determined by trends in heat capacity differences in Figure 7. In addition, the ordering of BDEs for bonds remains unchanged over the entire temperature range, and their relative values remain almost the same. Similar trends are observed for other isomers of butanol (Supporting Information Figure S3).

dx.doi.org/10.1021/jp501636r | J. Phys. Chem. A 2014, 118, 3039−3050

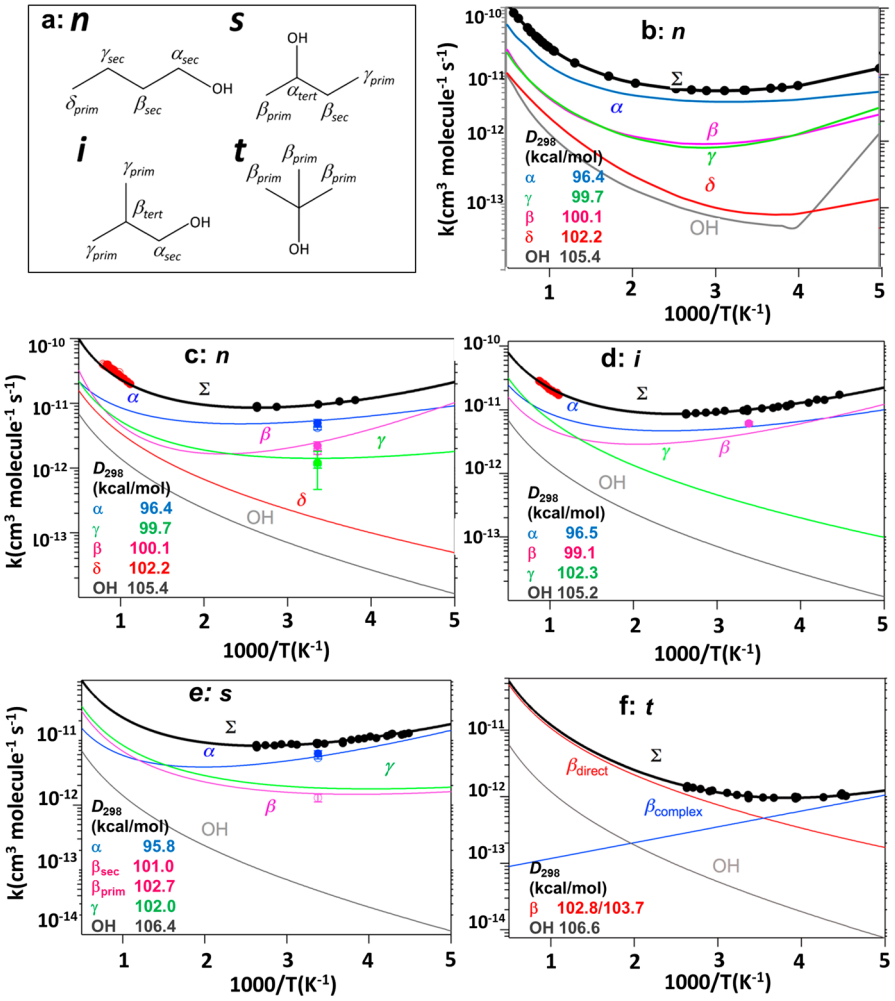

Figure 9. Total and site-specific rate constants (b)−(f) for H abstraction from the four butanol isomers (a), *n*-, iso- (labeled "*i*"), *sec*- (labeled "*s*"), and *tert*- (labeled "*t*"), by OH radical, from theoretical work of Seal et al.[56] (b) and experimental work of McGillen et al. (c)−(f),[54] along with MRACPF2 D_{298}s from Figure 6. $\beta_{complex}$ in the *tert*-butanol panel refers to formation of cyclic complexes whereas β_{direct} is a direct H abstraction (see ref 54). Σ refers to the total rate. (a), (c), (d), (e), and (f) are reprinted or adapted with permission from ref 54.

BDEs are commonly used to rationalize the relative ease of hydrogen abstraction from or decomposition of molecules, with the assumption that decomposition or abstraction is easier (faster) at bonds with lower BDEs. We test this intuitive idea by comparing site-specific rate constants for C−H abstraction against calculated BDEs. A limited set of experimental and computed rate constants are available for this comparison. Seal et al.[56] used multistructural variational transition state theory to compute theoretical hydrogen abstraction rate constants for *n*-butanol. Direct measurement of experimental rate constants for specific abstraction sites is rare; typically, only the total rate is recorded. Multiple sources of such total experimental rate constants for H-abstraction by OH are available for butanol isomers.[54] McGillen et al. extracted site-specific rates from total experimental rates by noting that total rates are a sum of site-specific rates assumed to have modified Arrhenius forms ($k_{total} = \sum_i A_i T^{n_i} e^{-E_i/kT}$). They fitted the modified Arrhenius parameters using measured total rates at different temperatures. The total rates and site-specific rates from Seal et al.'s theoretical calculations and McGillen et al.'s experimental data are shown in Figure 9b−f. We also display the various C−H and O−H MRACPF2 D_{298}s for each site.

The theoretical and experimental site-specific rates have crossovers. Thus, they do not support the assumption that a monotonic correspondence exists between BDEs and abstraction rates in all cases. Two exceptions do follow the conjectured relationship: apart from the crossover at low temperatures for the theoretical *n*-butanol OH site abstraction, O−H bonds generally have the lowest rates and the highest bond strengths, and primary C−H bonds in *n*-butanol have the next largest BDE along with the second lowest rate. We conclude that BDEs roughly correspond to rates for the strongest bonds, but not at all temperature ranges. It will be interesting to see how these correspondences change with more refined experimental data. It will also be useful to see how the trends are affected by the choice of abstractor radical as additional data become available.

6. CONCLUSIONS

We have computed BDEs of C1−C4 alcohols and aldehydes using a multireference averaged coupled-pair functional based scheme. We have explained the main origin of trends in these BDEs by analyzing geometry relaxation energies, which shows that trends in GREs correlate with trends in BDEs. Other factors, such as hyperconjugation and resonance stabilization, further refine the trends as well. C—H and C—C bonds α to OH in

dx.doi.org/10.1021/jp501636r | J. Phys. Chem. A 2014, 118, 3039−3050

alcohols are weakest among their respective bond types due to hyperconjugative stabilization of the resulting RCHOH radical when these bonds are broken. These α C—H and C—C bonds are therefore the most likely sites for respectively hydrogen abstraction and thermal decomposition of alcohols. Likewise, C—H and C—C bonds β to C═O in aldehydes are the weakest due to resonance stabilization of the resulting radical, and are the most likely sites for hydrogen abstraction and thermal decomposition of aldehydes. We also explored briefly the conjectured correspondence between BDEs and abstraction rates. Although bond-breaking processes with larger BDEs can be reasonably assumed to have lower rates, this assumption does not hold at all temperatures.

■ ASSOCIATED CONTENT

Supporting Information

Table S1 shows a comparison of BDEs and contributing terms when obtained from DFT-B3LYP/cc-pVTZ or DFT-B3LYP/6-311G(2d,p) geometries and vibrational frequencies. Table S2 shows Mulliken charges for H—C(═O)R bond breaking. Figures S1 and S2 compare GREs from DFT-B3LYP/cc-pVTZ and CCSD(T)/cc-pVTZ. Figure S3 shows D_T of C—H and O—H bonds in butanol isomers. This material is available free of charge via the Internet at http://pubs.acs.org.

■ AUTHOR INFORMATION

Corresponding Author

*E. A. Carter: e-mail: eac@princeton.edu; phone, +1 609 258 5391; fax, +1 609 258 5877.

Present Address

[⊥]Department of Chemical and Petroleum Engineering, Swanson School of Engineering, University of Pittsburgh, 804 Benedum Hall, 3700 O'Hara Street, Pittsburgh, PA 15261, United States.

Notes

The authors declare no competing financial interest.

■ ACKNOWLEDGMENTS

This work was supported as part of the Combustion Energy Frontier Research Center, an Energy Frontier Research Center funded by the U.S. Department of Energy, Office of Science, Basic Energy Sciences under Award Number DE-SC0001198. The work reported was performed on the TIGRESS high performance computer center at Princeton University, which is jointly supported by the Princeton Institute for Computational Science and Engineering and the Princeton University Office of Information Technology. We thank Dr. Gbenga Oyedepo for valuable discussions and David B. Krisiloff and Johannes M. Dieterich for critically reading our manuscript.

■ REFERENCES

(1) Agarwal, A. K. Biofuels (Alcohols and Biodiesel) Applications as Fuels for Internal Combustion Engines. *Prog. Energy Combust. Sci.* **2007**, *33*, 233−271, http://dx.doi.org/10.1016/j.pecs.2006.08.003.

(2) Sundarrajan, S.; Allakhverdiev, S. I.; Ramakrishna, S. Progress and Perspectives in Micro Direct Methanol Fuel Cell. *Int. J. Hydrogen Energy* **2012**, *37*, 8765−8786, http://dx.doi.org/10.1016/j.ijhydene.2011.12.017.

(3) Gonzalez, E. R.; Antolini, E., Direct Ethanol Fuel Cells: Catalysts. In *Encyclopedia of Electrochemical Power Sources*, Jürgen, G., Ed. Elsevier: Amsterdam, 2009; pp 402−411. http://dx.doi.org/10.1016/B978-044452745-5.00914-X.

(4) Wang, L. J. Production of Bioenergy and Bioproducts from Food Processing Wastes: A Review. *Trans. ASABE* **2013**, *56*, 217−229, http://dx.doi.org/10.13031/2013.42572.

(5) Burger, J. L.; Baibourine, E.; Bruno, T. J. Comparison of Diesel Fuel Oxygenate Additives to the Composition-Explicit Distillation Curve Method. Part 4: Alcohols, Aldehydes, Hydroxy Ethers, and Esters of Butanoic Acid. *Energy Fuels* **2011**, *26*, 1114−1123, http://dx.doi.org/10.1021/ef2016655.

(6) Jacobson, M. Z. Effects of Ethanol (E85) Versus Gasoline Vehicles on Cancer and Mortality in the United States. *Environ. Sci. Technol.* **2007**, *41*, 4150−4157, http://dx.doi.org/10.1021/es062085v.

(7) Kasper, T.; Oßwald, P.; Struckmeier, U.; Kohse-Höinghaus, K.; Taatjes, C. A.; Wang, J.; Cool, T. A.; Law, M. E.; Morel, A.; Westmoreland, P. R. Combustion Chemistry of the Propanol Isomers - Investigated by Electron Ionization and VUV-Photoionization Molecular-Beam Mass Spectrometry. *Combust. Flame* **2009**, *156*, 1181−1201, http://dx.doi.org/10.1016/j.combustflame.2009.01.023.

(8) Frassoldati, A.; Cuoci, A.; Faravelli, T.; Niemann, U.; Ranzi, E.; Seiser, R.; Seshadri, K. An Experimental and Kinetic Modeling Study of n-Propanol and Iso-Propanol Combustion. *Combust. Flame* **2010**, *157*, 2−16, http://dx.doi.org/10.1016/j.combustflame.2009.09.002.

(9) Veloo, P. S.; Dagaut, P.; Togbe, C.; Dayma, G.; Sarathy, S. M.; Westbrook, C. K.; Egolfopoulos, F. N. Jet-Stirred Reactor and Flame Studies of Propanal Oxidation. *Proc. Combust. Inst.* **2013**, *34*, 599−606, http://dx.doi.org/10.1016/j.proci.2012.06.138.

(10) Veloo, P. S.; Dagaut, P.; Togbé, C.; Dayma, G.; Sarathy, S. M.; Westbrook, C. K.; Egolfopoulos, F. N. Experimental and Modeling Study of the Oxidation of N and Iso-Butanal. *Combust. Flame* **2013**, *160*, 1609−1626, http://dx.doi.org/10.1016/j.combustflame.2013.03.018.

(11) Oyeyemi, V. B.; Krisiloff, D. B.; Keith, J. A.; Libisch, F.; Pavone, M.; Carter, E. A. Size-Extensivity-Corrected Multireference Configuration Interaction Schemes to Accurately Predict Bond Dissociation Energies of Oxygenated Hydrocarbons. *J. Chem. Phys.* **2014**, *140*, 044317−044328, http://dx.doi.org/10.1063/1.4862159.

(12) Oyeyemi, V. B.; Keith, J. A.; Carter, E. A. Accurate Bond Energies of Biodiesel Methyl Esters from Multireference Averaged Coupled-Pair Functional Calculations. *J. Phys. Chem. A* **2014**, http://dx.doi.org/10.1021/jp412727w.

(13) Coote, M.; Pross, A.; Radom, L., Understanding Alkyl Substituent Effects in R-O Bond Dissociation Reactions in Open- and Closed-Shell Systems. In *Fundamental World of Quantum Chemistry*; Brändas, E., Kryachko, E., Eds.; Springer: Netherlands, 2004; pp 563−579, DOI http://dx.doi.org/10.1007/978-94-017-0448-9_24.

(14) Izgorodina, E. I.; Coote, M. L.; Radom, L. Trends in R−X Bond Dissociation Energies (R = Me, Et, i-Pr, t-Bu; X = H, CH_3, OCH_3, OH, F): A Surprising Shortcoming of Density Functional Theory. *J. Phys. Chem. A* **2005**, *109*, 7558−7566, http://dx.doi.org/10.1021/jp052021r.

(15) da Silva, G.; Chen, C.-C.; Bozzelli, J. W. Bond Dissociation Energy of the Phenol OH Bond from Ab Initio Calculations. *Chem. Phys. Lett.* **2006**, *424*, 42−45, http://dx.doi.org/10.1016/j.cplett.2006.04.022.

(16) da Silva, G.; Kim, C.-H.; Bozzelli, J. W. Thermodynamic Properties (Enthalpy, Bond Energy, Entropy, and Heat Capacity) and Internal Rotor Potentials of Vinyl Alcohol, Methyl Vinyl Ether, and Their Corresponding Radicals. *J. Phys. Chem. A* **2006**, *110*, 7925−7934, http://dx.doi.org/10.1021/jp0602878.

(17) Black, G.; Curran, H. J.; Pichon, S.; Simmie, J. M.; Zhukov, V. Bio-Butanol: Combustion Properties and Detailed Chemical Kinetic Model. *Combust. Flame* **2010**, *157*, 363−373, http://dx.doi.org/10.1016/j.combustflame.2009.07.007.

(18) El-Nahas, A. M.; Mangood, A. H.; El-Meleigy, A. B. A Computational Study on the Structures and Energetics of Isobutanol Pyrolysis. *Comput. Theor. Chem.* **2012**, *997*, 94−102, http://dx.doi.org/10.1016/j.comptc.2012.08.009.

(19) Ochterski, J. W.; Petersson, G. A.; Montgomery, J. A., Jr. A Complete Basis Set Model Chemistry. V. Extensions to Six or More Heavy Atoms. *J. Chem. Phys.* **1996**, *104*, 2598−2619, http://dx.doi.org/10.1063/1.470985.

(20) da Silva, G.; Bozzelli, J. W. Enthalpies of Formation, Bond Dissociation Energies, and Molecular Structures of the n-Aldehydes

(Acetaldehyde, Propanal, Butanal, Pentanal, Hexanal, and Heptanal) and Their Radicals. *J. Phys. Chem. A* **2006**, *110*, 13058−13067, http://dx.doi.org/10.1021/jp063772b.
(21) Gdanitz, R. J.; Ahlrichs, R. The Averaged Coupled-Pair Functional (ACPF): A Size-Extensive Modification of MR CI(SD). *Chem. Phys. Lett.* **1988**, *143*, 413−420, http://dx.doi.org/10.1016/0009-2614(88)87388-3.
(22) Gdanitz, R. J. A New Version of the Multireference Averaged Coupled-Pair Functional (MR-ACPF-2). *Int. J. Quantum Chem.* **2001**, *85*, 281−300, http://dx.doi.org/10.1002/qua.10019.
(23) Becke, A. D. Density-Functional Thermochemistry 0.3. The Role of Exact Exchange. *J. Chem. Phys.* **1993**, *98*, 5648−5652, http://dx.doi.org/10.1063/1.464913.
(24) Ditchfield, R.; Hehre, W. J.; Pople, J. A. Self-Consistent Molecular-Orbital Methods. IX. An Extended Gaussian-Type Basis for Molecular-Orbital Studies of Organic Molecules. *J. Chem. Phys.* **1971**, *54*, 724−728, http://dx.doi.org/10.1063/1.1674902.
(25) Schmidt, M. W.; Baldridge, K. K.; Boatz, J. A.; Elbert, S. T.; Gordon, M. S.; Jensen, J. H.; Koseki, S.; Matsunaga, N.; Nguyen, K. A.; Su, S.; et al. General Atomic and Molecular Electronic Structure System. *J. Comput. Chem.* **1993**, *14*, 1347−1363, http://dx.doi.org/10.1002/jcc.540141112.
(26) Dunning, T. Gaussian Basis Sets for Use in Correlated Molecular Calculations. I. The Atoms Boron Through Neon and Hydrogen. *J. Chem. Phys.* **1989**, *90*, 1007−1024, http://dx.doi.org/10.1063/1.456153.
(27) NIST Computational Chemistry Comparison and Benchmark DataBase. http://cccbdb.nist.gov/.
(28) Siegbahn, P. E. M. Multiple Substitution Effects in Configuration Interaction Calculations. *Chem. Phys. Lett.* **1978**, *55*, 386−394, http://dx.doi.org/10.1016/0009-2614(78)87046-8.
(29) Szabo, A.; Ostlund, N. S. *Modern Quantum Chemistry: Introduction to Advanced Electronic Structure Theory*; McGraw-Hill: New York, 1989; p 480.
(30) Brueckner, K. A. Many-Body Problem for Strongly Interacting Particles. II. Linked Cluster Expansion. *Phys. Rev.* **1955**, *100*, 36−45, http://dx.doi.org/10.1103/PhysRev.100.36.
(31) Luken, W. L. Unlinked Cluster Corrections for Configuration Interaction Calculations. *Chem. Phys. Lett.* **1978**, *58*, 421−424, http://dx.doi.org/10.1016/0009-2614(78)85066-0.
(32) Davidson, E. R.; Silver, D. W. Size Consistency in the Dilute Helium Gas Electronic Structure. *Chem. Phys. Lett.* **1977**, *52*, 403−406, http://dx.doi.org/10.1016/0009-2614(77)80475-2.
(33) Duch, W.; Diercksen, G. H. F. Size-Extensivity Corrections in Configuration Interaction Methods. *J. Chem. Phys.* **1994**, *101*, 3018−3030, http://dx.doi.org/10.1063/1.467615.
(34) Roos, B. O., The Complete Active Space Self-Consistent Field Method and Its Applications in Electronic Structure Calculations. In *Advances in Chemical Physics: Ab Initio Methods in Quantum Chemistry - Part 2*; Lawley, K. P., Ed.; John Wiley & Sons: New York, 1987; Vol. *69*, pp 399−445, DOI http://dx.doi.org/10.1002/9780470142943.ch7.
(35) Oyeyemi, V. B.; Pavone, M.; Carter, E. A. Accurate Bond Energies of Hydrocarbons from Complete Basis Set Extrapolated Multi-Reference Singles and Doubles Configuration Interaction. *ChemPhysChem* **2011**, *12*, 3354−3364, http://dx.doi.org/10.1002/cphc.201100447.
(36) Truhlar, D. G. Basis-Set Extrapolation. *Chem. Phys. Lett.* **1998**, *294*, 45−48, http://dx.doi.org/10.1016/S0009-2614(98)00866-5.
(37) Fast, P. L.; Sanchez, M. L.; Truhlar, D. G. Infinite Basis Limits in Electronic Structure Theory. *J. Chem. Phys.* **1999**, *111*, 2921−2926, http://dx.doi.org/10.1063/1.479659.
(38) Aquilante, F.; De Vico, L.; Ferré, N.; Ghigo, G.; Malmqvist, P.; Neogrády, P.; Pedersen, T. B.; Pitoňák, M.; Reiher, M.; Roos, B. O.; et al. MOLCAS 7: The Next Generation. *J. Comput. Chem.* **2010**, *31*, 224−247, http://dx.doi.org/10.1002/jcc.21318.
(39) Walter, D.; Venkatnathan, A.; Carter, E. A. Local Correlation in the Virtual Space in Multireference Singles and Doubles Configuration Interaction. *J. Chem. Phys.* **2003**, *118*, 8127−8139, http://dx.doi.org/10.1063/1.1565314.
(40) Chwee, T. S.; Szilva, A. B.; Lindh, R.; Carter, E. A. Linear Scaling Multireference Singles and Doubles Configuration Interaction. *J. Chem. Phys.* **2008**, *128*, 224106−224114, http://dx.doi.org/10.1063/1.2937443.
(41) Chwee, T. S.; Carter, E. A. Cholesky Decomposition Within Local Multireference Singles and Doubles Configuration Interaction. *J. Chem. Phys.* **2010**, *132*, 074104−074113, http://dx.doi.org/10.1063/1.3315419.
(42) Krisiloff, D.; Carter, E. A. Approximately Size Extensive Local Multireference Singles and Doubles Configuration Interaction. *Phys. Chem. Chem. Phys.* **2012**, *14*, 7710−7717, http://dx.doi.org/10.1039/C2CP23757A.
(43) Krisiloff, D. B.; Dieterich, J. M.; Libisch, F.; Carter, E. A., Numerical Challenges in a Cholesky-Decomposed Local Correlation Quantum Chemistry Framework. In *Mathematical and Computational Modeling with Applications*; Melnick, R., Ed.; Wiley: New York, in press.
(44) Bartlett, R. J.; Purvis, G. D. Many-Body Perturbation Theory, Coupled-Pair Many-Electron Theory, and the Importance of Quadruple Excitations for the Correlation Problem. *Int. J. Quantum Chem.* **1978**, *14*, 561−581, http://dx.doi.org/10.1002/qua.560140504.
(45) Werner, H.-J.; Knowles, P. J.; Knizia, G.; Manby, F. R.; Schütz, M. MOLPRO: A General-Purpose Quantum Chemistry Program Package. *WIREs Comput. Mol. Sci.* **2012**, *2*, 242−253, http://dx.doi.org/10.1002/wcms.82.
(46) Montgomery, J. A.; Frisch, M. J.; Ochterski, J. W.; Petersson, G. A. A Complete Basis Set Model Chemistry. VI. Use of Density Functional Geometries and Frequencies. *J. Chem. Phys.* **1999**, *110*, 2822−2827, http://dx.doi.org/10.1063/1.477924.
(47) Hehre, W. J.; Ditchfield, R.; Radom, L.; Pople, J. A. Molecular Orbital Theory of the Electronic Structure of Organic Compounds. V. Molecular Theory of Bond Separation. *J. Am. Chem. Soc.* **1970**, *92*, 4796−4801, http://dx.doi.org/10.1021/ja00719a006.
(48) Wodrich, M. D.; Corminboeuf, C.; Wheeler, S. E. Accurate Thermochemistry of Hydrocarbon Radicals Via an Extended Generalized Bond Separation Reaction Scheme. *J. Phys. Chem. A* **2012**, *116*, 3436−3447, http://dx.doi.org/10.1021/jp212209q.
(49) Luo, Y.-R. *Comprehensive Handbook of Chemical Bond Energies*; CRC Press: Boca Raton, FL, 2007; DOI http://dx.doi.org/10.1201/9781420007282.
(50) Ruscic, B.; Pinzon, R. E.; Morton, M. L.; von Laszevski, G.; Bittner, S. J.; Nijsure, S. G.; Amin, K. A.; Minkoff, M.; Wagner, A. F. Introduction to Active Thermochemical Tables: Several "Key" Enthalpies of Formation Revisited. *J. Phys. Chem. A* **2004**, *108*, 9979−9997, http://dx.doi.org/10.1021/jp047912y.
(51) Ruscic, B.; Pinzon, R. E.; von Laszevski, G.; Kodeboyina, D.; Burcat, A.; Leahy, D.; Montoy, D.; Wagner, A. F. Active Thermochemical Tables: Thermochemistry for the 21st Century. *J. Phys.: Conf. Ser.* **2005**, *16*, 561−570, http://dx.doi.org/10.1088/1742-6596/16/1/078.
(52) Klippenstein, S. J.; Harding, L. B.; Ruscic, B., Ab initio Computations and Active Thermochemical Tables Hand in Hand: Heats of Formation of Core Combustion Species. *J. Phys. Chem. A*, to be submitted.
(53) Lecture notes of William A. Goddard, III. Relevant sections can be accessed at http://www.wag.caltech.edu/home/ch120/Slides/L6-jan18-2012.pdf, pp 10−17.
(54) McGillen, M. R.; Baasandorj, M.; Burkholder, J. B. Gas-Phase Rate Coefficients for the OH + n-, i-, s-, and t-Butanol Reactions Measured Between 220 and 380 K: Non-Arrhenius Behavior and Site-Specific Reactivity. *J. Phys. Chem. A* **2013**, *117*, 4636−4656, http://dx.doi.org/10.1021/jp402702u.
(55) McQuarrie, D.; Simon, J. *Molecular Thermodynamics*; University Science Books: Mill Valley, CA, 1999.
(56) Seal, P.; Oyedepo, G.; Truhlar, D. G. Kinetics of the Hydrogen Atom Abstraction Reactions from 1-Butanol by Hydroxyl Radical: Theory Matches Experiment and More. *J. Phys. Chem. A* **2012**, *117*, 275−282, http://dx.doi.org/10.1021/jp310910f.